

## Review Article

# Highly Protein-resistant AuNPs-ampholytes Modified Boric Acid Hydrogel for Saliva Glucose Detection

Qian Dou<sup>1,2\*</sup>, Tingjun Chen<sup>1,2</sup>, Liping Zhu<sup>3</sup>, Qing Dai<sup>1,2</sup> and Debo Hu<sup>1,2\*</sup>

<sup>1</sup>CAS Key Laboratory of Nanophotonic Materials and Devices, CAS Key Laboratory of Standardization and Measurement for Nanotechnology, National Center for Nanoscience and Technology, Beijing 100190, China

<sup>2</sup>Center of Materials Science and Optoelectronics Engineering, University of Chinese Academy of Sciences, Beijing 100049, China

<sup>3</sup>School of Materials Science and Engineering, Zhengzhou University, Zhengzhou 450001, P. R. China

**Received:** 17 March, 2025

**Accepted:** 24 March, 2025

**Published:** 25 March, 2025

**\*Corresponding authors:** Qian Dou, CAS Key Laboratory of Nanophotonic Materials and Devices, CAS Key Laboratory of Standardization and Measurement for Nanotechnology, National Center for Nanoscience and Technology, Beijing 100190, China, E-mail: douq@nanoctr.cn

Debo Hu, CAS Key Laboratory of Nanophotonic Materials and Devices, CAS Key Laboratory of Standardization and Measurement for Nanotechnology, National Center for Nanoscience and Technology, Beijing 100190, China, E-mail: hudb@nanoctr.cn

**Keywords:** QCM; Saliva glucose; Antifouling materials; Boric acid hydrogel; Gold nanoparticles (AuNPs)

**Copyright License:** © 2025 Dou Q, et al. This is an open-access article distributed under the terms of the Creative Commons Attribution License, which permits unrestricted use, distribution, and reproduction in any medium, provided the original author and source are credited.

<https://www.chemisgroup.us>



## Abstract

Saliva glucose detection using QCM technology has garnered significant attention of non-invasive blood glucose monitoring. Introducing antifouling materials is a pivotal strategy for addressing the issue of indiscriminate protein adsorption in saliva. Nonetheless, equipping surfaces with antifouling properties often comes at the cost of compromising the sensitivity of QCM tests. To tackle this challenge, we engineered an innovative antifouling hydrogel that integrates gold nanoparticles functionalized with L-cysteine (Au-Cys). When immobilized on quartz chips, this hydrogel not only enhanced glucose sensitivity but also significantly reduced nonspecific protein adsorption. The sensitivity of hydrogels without Au-Cys increased from 0.34 Hz/(mg/L) to 0.45 Hz/(mg/L) of hydrogels containing Au-Cys. Additionally, protein adhesion of bovine serum albumin, lysozyme, and mucin was markedly decreased by approximately 25, 10, and 50 times, respectively.

## Abbreviations

QCM: Quartz Crystal Microbalance; Au: Gold Nanoparticles; Cys: L-cysteine; Au-Cys: Gold Nanoparticles Functionalized with L-cysteine

## Introduction

Diabetes is one of the biggest health problems facing humanity in the 21st century, characterized by high incidence rates, high mortality rates, high costs, and high rates of undiagnosed cases [1,2]. According to the International Diabetes Federation, as of 2019, 463 million people (aged 20–79) worldwide are suffering from diabetes. Among them, the number of diagnosed cases in China has reached 116.4 million, ranking first in the world [3]. Strict control of blood

glucose can significantly reduce the risk of diabetes-related complications, highlighting the need for regular blood glucose monitoring [4]. Blood glucose testing typically requires finger pricks or other invasive methods, such as Continuous Glucose Monitoring Systems (CGMS) [5,6]. These methods are painful, inconvenient and carry infection risks, leading to poor patient compliance [7,8]. To address this challenge, saliva-based glucose monitoring has emerged as a promising alternative. Research has consistently demonstrated a strong correlation between salivary and blood glucose levels, making it an ideal non-invasive biomarker for diabetes management [9–11].

Quartz Crystal Microbalance (QCM) is an extremely sensitive mass sensor capable of detecting mass changes at the nanogram level [12,13]. Due to its simple structure, low cost, label-free nature, and real-time measurement capabilities,

it is considered an ideal tool for detecting salivary glucose concentration [14,15]. The glucose detection technology based on QCM involves designing a glucose-sensitive film on the surface of the crystal chip, which detects glucose through the specific reversible binding between the film and glucose [16,17]. However, when using saliva as a sample for glucose monitoring, the main challenge lies in the highly complex composition of saliva, with extremely low levels of glucose (only 1/100 to 1/20 of blood glucose levels [18,19]) and very high levels of macromolecular proteins (71–2232 mg/L [20]). When the QCM sensor is exposed to saliva samples, the large signal generated by the non-specific adsorption of high-content proteins on the film can make it difficult to effectively identify the weak signal produced by the binding of trace amounts of glucose. Therefore, to achieve effective and accurate detection of salivary glucose, it is necessary to eliminate the interference from non-specific protein adsorption in saliva. To address this issue, constructing antifouling sensors based on functional materials is an effective solution [21]. For example, Yang, et al. [22] developed a zwitterionic hydrogel using polycarboxybetaine methacrylate (polyCBMA) as a base material for electrochemical glucose biosensors to detect glucose in complex media. The results showed that sensors coated with polyCBMA hydrogel by chemical methods exhibited good sensitivity and a linear response to glucose in PBS, 10%, 50%, and 100% human serum. Hu, et al. [23] polymerized the zwitterionic sulfobetaine methacrylate (SBMA) monomer on the surface of enzyme-adsorbed electrodes. The results indicated that the polymer brush coating reduced non-specific protein adsorption by more than 99%, and after 15 days, the sensor's sensitivity remained at 94%. While successful in blood glucose detection, their application to salivary glucose remains limited due to the trade-off between antifouling properties and sensitivity. Developing novel antifouling materials tailored to the unique characteristics of saliva is crucial for advancing QCM-based salivary glucose monitoring [24,25].

We have successfully developed a novel salivary glucose sensor incorporating an antifouling hydrogel. The hydrogel, composed of gold nanoparticles (AuNPs) functionalized with L-cysteine (Cys), demonstrated enhanced glucose detection sensitivity and resistance to protein fouling. The strong Au-S bond facilitated the self-assembly of AuNPs and Cys, leading to a robust and biocompatible composite material. When integrated into a boronic acid hydrogel, this composite significantly improved the sensor's performance in detecting salivary glucose under physiological conditions. Compared to sensors without the antifouling material, the response signal to glucose was 1.3 times higher, while maintaining excellent resistance to bovine serum albumin, lysozyme, and mucin. These findings highlight the potential of our approach for developing reliable and practical non-invasive saliva glucose sensors.

## Experimental section

### Reagents

N-Vinylpyrrolidone (NVP, 99%), acrylamide (AM, 98.5%), and ethylene glycol dimethacrylate (EGDMA,

98%) were purchased from Shanghai Macklin Biochemical Co., Ltd. 2,2-Dimethoxy-2-phenylacetophenone (DMPA, > 98%) was obtained from TCI (Shanghai) Development Co., Ltd. 3-Aminopropyltriethoxysilane (APTES, 98%) was acquired from Alfa Aesar (China) Chemical Co., Ltd. 3-Acrylamidophenylboronic acid (3-APB, 98%) was sourced from Tianjin Heowns Biochemical Technology Co., Ltd. N,N'-Methylenebisacrylamide (BIS, 98%) was obtained from Sinopharm Chemical Reagent Co., Ltd. Dimethyl sulfoxide (DMSO), glucose, L-cysteine, maleic anhydride, bovine serum albumin (BSA), lysozyme (LYS), mucin (MUC), and other chemicals were all analytical grade reagents.

### Instruments

Glucose and antifouling tests were conducted using the QCM 200 (SRS). The surface morphology of the materials was studied using a scanning electron microscope (S-4800). The functional groups of the materials were determined using a micro-IR spectrometer (SP-200i). The chemical composition of the hydrogel was analyzed by X-ray photoelectron spectrometry (ESCALAB250- Xi). The pressure involved in the hydrogel preparation process was provided by a lab-built pressing machine. UV polymerization was carried out using a UV lamp (365 nm, with a maximum power of 3 W).

### Synthesis of smart hydrogel

**Surface modification of QCM chips:** The QCM chips were ultrasonicated for 10 minutes in a piranha solution (a mixture of  $\text{H}_2\text{SO}_4$  (96% w/w) and  $\text{H}_2\text{O}_2$  (30% w/w) at a volume ratio of 7:3). After treatment, the chips were rinsed with distilled water and dried with nitrogen gas. The chips were then placed in a mixed solution of 3-aminopropyltriethoxysilane (100  $\mu\text{L}$ ) and ethanol (50 mL). After reacting at room temperature for 12 hours, the chips were repeatedly rinsed with ethanol and dried with nitrogen gas. The treated chips were then soaked in a mixed solution of maleic anhydride (1 g) and dimethylformamide (50 mL) and reacted at room temperature for 12 hours. Finally, the chips were rinsed with ethanol and dried with nitrogen gas [21].

**Synthesis of Au-Cys:** Citrate-protected gold nanoparticles were dispersed in a mixed ethanol-water solution containing an excess of L-cysteine. The ethanol content was maintained at 30% or less of the total volume. After a 24-hour reaction at room temperature, the resulting AuNPs-Cys composite was thoroughly washed with distilled water and dried for subsequent use [21].

**Deposition of Au-Cys-hydrogel on the chip:** A pre-polymerization solution was prepared by combining 0.3 mg Au-Cys, 17.2 mg 3-APB, 1.5 mg BIS, 27.7 mg AM, 2.6 mg DMPA, and 10  $\mu\text{L}$  NVP in 100  $\mu\text{L}$  dimethyl sulfoxide [21]. Twenty-five microliters of this solution were then dropped onto a 10 x 10 cm quartz plate. The chip was placed face down on the solution, firmly pressed and exposed to UV light for 1 hour. The hydrogel-coated chip was subsequently separated from the quartz plate by immersing it in distilled water and thoroughly washed [26]. The hydrogel synthesized using this composition formula is designated as Au-Cys-hydrogel.

**Deposition of hydrogel without Au-Cys on the chip:** A pre-polymerization solution was prepared by combining 17.2 mg 3-APB, 1.5 mg BIS, 27.7 mg AM, 2.6 mg DMPA, and 10  $\mu$ L NVP in 100  $\mu$ L dimethyl sulfoxide. Twenty-five microliters of this solution were then dropped onto a 10x10 cm quartz plate. The chip was placed face down on the solution, pressed firmly, and exposed to UV light for 1 hour. The hydrogel-coated chip was subsequently separated from the quartz plate by immersing it in distilled water and thoroughly washed. The hydrogel synthesized using this composition formula is designated as hydrogel.

### Glucose sensor testing

The hydrogel-coated QCM chip was dried with nitrogen gas and then placed in the QCM reaction chamber. A peristaltic pump was used to introduce the test solution into the chamber while continuously monitoring the QCM frequency in real-time using specialized software. Once the frequency change ( $\Delta F$ ) stabilized, the hydrogel's response to glucose and its antifouling properties were evaluated [21]. During each experiment, a 2 mL sample dissolved in Phosphate-Buffered Saline (PBS) was injected at a flow rate of 200  $\mu$ L/s. After complete injection, the peristaltic pump was stopped, and the system was allowed to stabilize before introducing the next sample. Except for the pH tests conducted at pH 6.8, 7.2, and 7.5, all other QCM performance tests were performed at pH 7.2.

## Results and discussion

### Synthesis of Au-Cys-hydrogel

As mentioned in the introduction, the key obstacle in developing QCM-based salivary glucose sensors is the need to overcome the interference of high-concentration proteins while maintaining sensitivity to low levels of glucose. The design of antifouling glucose-sensitive hydrogels is therefore paramount for the successful implementation of such sensors.

Currently, anti-protein materials mainly include polyethylene glycol (PEG) [27] zwitterionic polymers [28]

peptides and polypeptides [29] zwitterionic electrolytes (natural amino acids Arg<sup>+</sup>, Cys<sup>+</sup>, Asp<sup>-</sup> and Glu<sup>-</sup>, N<sup>+</sup>(CH<sub>3</sub>)<sub>3</sub> and -SO<sub>3</sub><sup>-</sup>/-COO<sup>-</sup>)<sub>30</sub>. Among them, natural amino acids, due to their zwitterionic nature, biomimetic properties, excellent chemical stability, convenient sourcing, and outstanding antifouling properties, have attracted widespread attention from researchers [30,31]. Particularly, L-cysteine (Cys), one of over 20 natural amino acids, is the only substance containing a thiol group (SH), which can be used for the modification of various materials [32]. Gold nanoparticles (AuNPs), with their high surface-to-volume ratio, provide a means for signal amplification [33,34].

Based on this, a simple and efficient anti-contamination saliva glucose sensor is designed. Cys was grafted onto AuNPs via Au-S bonds to create an antifouling composite material. This composite was then incorporated into a hydrogel pre-polymerization solution and subsequently synthesized onto a double-bond modified QCM chip using UV pressing-assisted polymerization, resulting in the formation of the Au-Cys-hydrogel sensor [26].

As illustrated in Figure 1, when the sample solution is introduced onto the chip surface, the boronic acid functional groups within the hydrogel matrix undergo specific and reversible binding with glucose molecules. Simultaneously, the cysteine-modified gold nanoparticles (Au-Cys) effectively minimize nonspecific protein adsorption through their steric hindrance and hydrophilic properties, thereby eliminating potential interference from biological contaminants on the detection signal. This dual-function mechanism endows the sensor with remarkable selectivity and reliable detection performance, ensuring highly sensitive and accurate glucose quantification.

### Material characterization

To verify the effectiveness of the synthesis of Au-Cys-hydrogel and to further understand the microscopic morphological characteristics of this material, we characterized

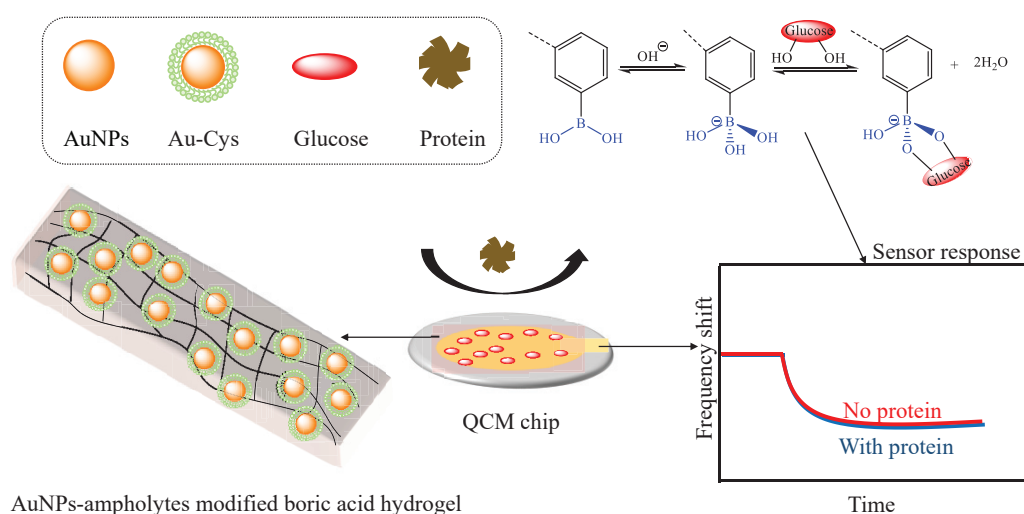


**Figure 1:** The preparation and identification process of saliva glucose sensor.



and analyzed its properties using an infrared absorption spectrometer, X-ray Photoelectron Spectroscopy (XPS), and Scanning Electron Microscope (SEM) separately.

First, the Au-Cys and Au-Cys-hydrogel were characterized using an infrared spectrometer. As shown in Figure 2a-i, the blue curve represents the infrared absorption spectrum of Au-Cys. The peak appearing at  $\sim 3022\text{ cm}^{-1}$  is attributed to the symmetric stretching vibration absorption of  $-\text{NH}_2$ . The stretching and bending absorption peaks of  $\text{NH}_3^+$  appear at  $\sim 2919\text{ cm}^{-1}$  and  $\sim 1578\text{ cm}^{-1}$ , respectively. Meanwhile, the peaks of the asymmetric and symmetric stretching vibrations of  $\text{COO}^-$  appear at  $\sim 1618\text{ cm}^{-1}$  and  $\sim 1483\text{ cm}^{-1}$ , respectively. The peak at  $\sim 772\text{ cm}^{-1}$  indicates the formation of the Au-S bond [35]. Since Cys is a zwitterionic molecule, the absorption peaks of  $\text{NH}_3^+$  and  $\text{COO}^-$  originate from the partial protonation and ionization of  $\text{NH}_2$  and  $\text{COOH}$  on Cys. These results ultimately confirm the successful grafting of Cys onto the surface of AuNPs. Figure 2a-ii, the red curve represents the infrared absorption spectrum of Au-Cys-hydrogel. The absorption peaks at  $\sim 3318\text{ cm}^{-1}$  and  $\sim 3193\text{ cm}^{-1}$  correspond to the asymmetric and symmetric vibrations of H-NCO. The peak at  $\sim 1653\text{ cm}^{-1}$  is attributed to C=O stretching. The characteristic absorption peak of  $\text{C}_6\text{H}_6$

appears at  $\sim 1421\text{ cm}^{-1}$ . The absorption peak at  $\sim 1342\text{ cm}^{-1}$  is assigned to  $\text{B(OH)}_2$  [36]. The appearance of these absorption peaks confirms the formation of the boronic acid hydrogel.

C 1s peak at 284.8 eV from Au-Cys-poly(acrylamide-co-3APB) hydrogel was used as a reference, using Gaussian-Lorentzian peak profiles after the Shirley background subtraction to get the peaks of Au 4f<sub>7/2,5/2</sub>, S 2p<sub>3/2,1/2</sub>, and B 1s (Figure 2b). The Au 4f<sub>7/2</sub> and 4f<sub>5/2</sub> signal at 84.2 eV and 87.9 eV, the S 2p<sub>3/2</sub> and S 2p<sub>1/2</sub> signal at 163.5 eV and 168.0 eV indicate the presence of Au-Cys in boronic acid hydrogel [37,38]. The B 1s signal at 191.4 eV indicates the presence of boronic acid groups [26].

Furthermore, the surface morphology of the Au-Cys and Au-Cys-hydrogel-coated chips were characterized using Scanning Electron Microscopy (SEM). Au-Cys was dispersed in ethanol solution and then dropped onto a single crystal silicon (111) surface. After the solvent evaporated, the samples were directly observed under SEM. Figure 2c-i shows that Au-Cys are in a clustered state. From the top view of the hydrogel-coated chip (Figure 2c-ii), it can be clearly seen that Au-Cys

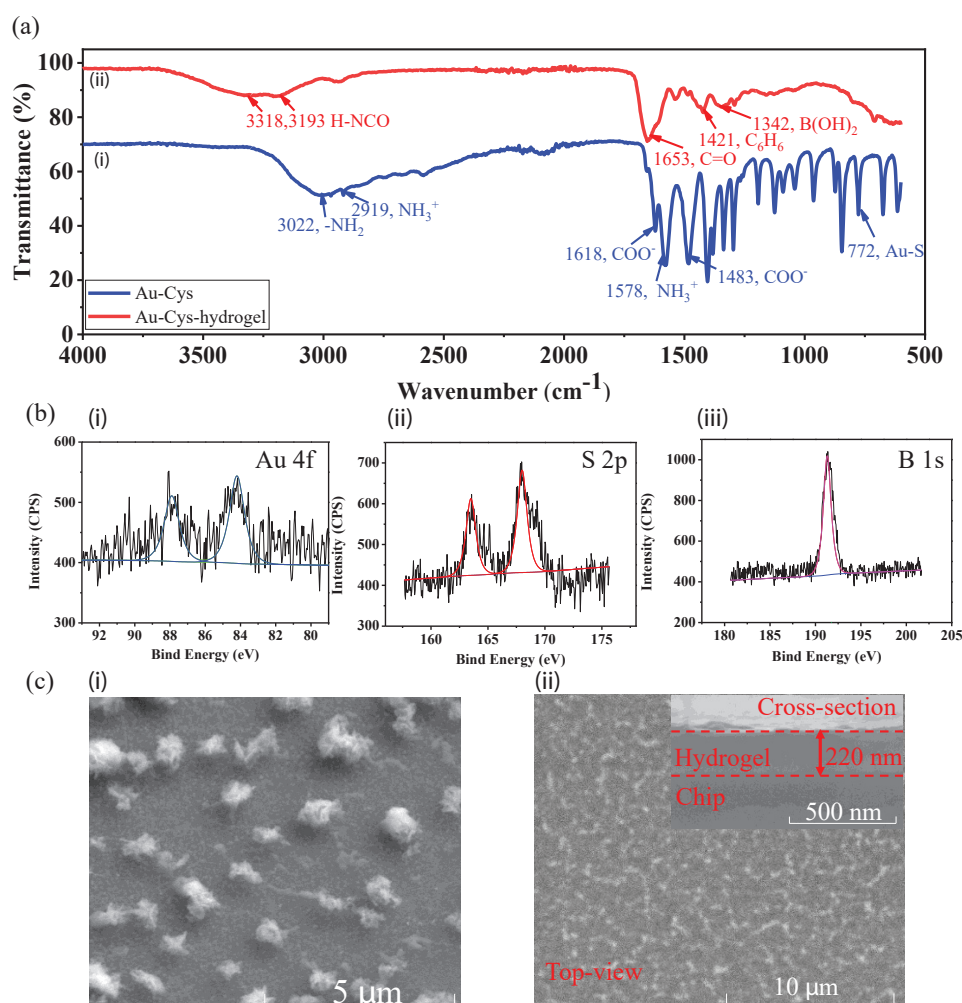


**Figure 2:** Characterization. (a) FTIR spectra of Au-Cys and Au-Cys-poly(acrylamide-co-3APB) hydrogel. (b) The XPS spectra of Au4fS2p and B1s. (c) The SEM of Au-Cys and Au-Cys-poly(acrylamide-co-3APB) hydrogel.

are uniformly dispersed within the hydrogel. The cross-sectional image reveals that the Au-Cys-hydrogel exhibits a dense microstructure with a thickness of approximately 220 nm.

## The responsiveness to glucose

Theoretically, the concentration of glucose in saliva is 1/100 to 1/50 of the blood glucose concentration [39,40], ranging from 2 to 120 mg/L. As illustrated in Figure 3a, as the glucose concentration increases,  $\Delta F$  gradually decreases. Conversely, as the glucose concentration decreases,  $\Delta F$  gradually increases. For the same glucose concentration,  $\Delta F$  is almost identical. Within the glucose concentration range of 0 to 200 mg/L, the Au-Cys-hydrogel demonstrates excellent responsiveness to glucose.

The response of Au-Cys-hydrogel to glucose was tested under different pH conditions (6.8 to 7.5, covering the physiological pH range of saliva). As shown in Figure 3b, with an increase in pH value, the absolute value of the corresponding  $\Delta F$  gradually increases. This suggests that a slightly elevated pH can improve glucose sensitivity. The reason is that a higher pH promotes the hydrolysis of phenylboronic acid groups, allowing more boronic acid groups to bind with glucose.

Additionally, the figure shows a good linear relationship between glucose concentration and  $\Delta F$  at the same pH value, with linear correlation coefficients of 0.9938 (pH 6.8), 0.9553 (pH 7.2), and 0.9908 (pH 7.5).

It is known that the thickness of the hydrogel influences the sensitivity of the glucose QCM sensor [41]. Thus, different film thicknesses on glucose detection were studied. As can be seen from Figure 3c, the absolute value of response frequency increases gradually with the increase of film thickness. This means that the hydrogel swell, and more glucose molecules will be adsorbed to the surface of the sensor [26]. If the film thickness is greater than 830 nm, the QCM device is easy to stop vibration and cannot continue to work.

One of the greatest advantages of the reaction between glucose and phenylboronic acid is its reversibility [42]. This means that continuous glucose monitoring can be achieved during actual measurements without any washing or regeneration steps. To demonstrate the reversibility of our Au-Cys-hydrogel, we conducted repeated testing-elution cycles at a pH of 7.2, alternating between glucose concentrations of 0 and 200 mg/L. As shown in Figure 3d, the hydrogel exhibited complete reversibility throughout 10 cycles, indicating its suitability for continuous glucose monitoring.

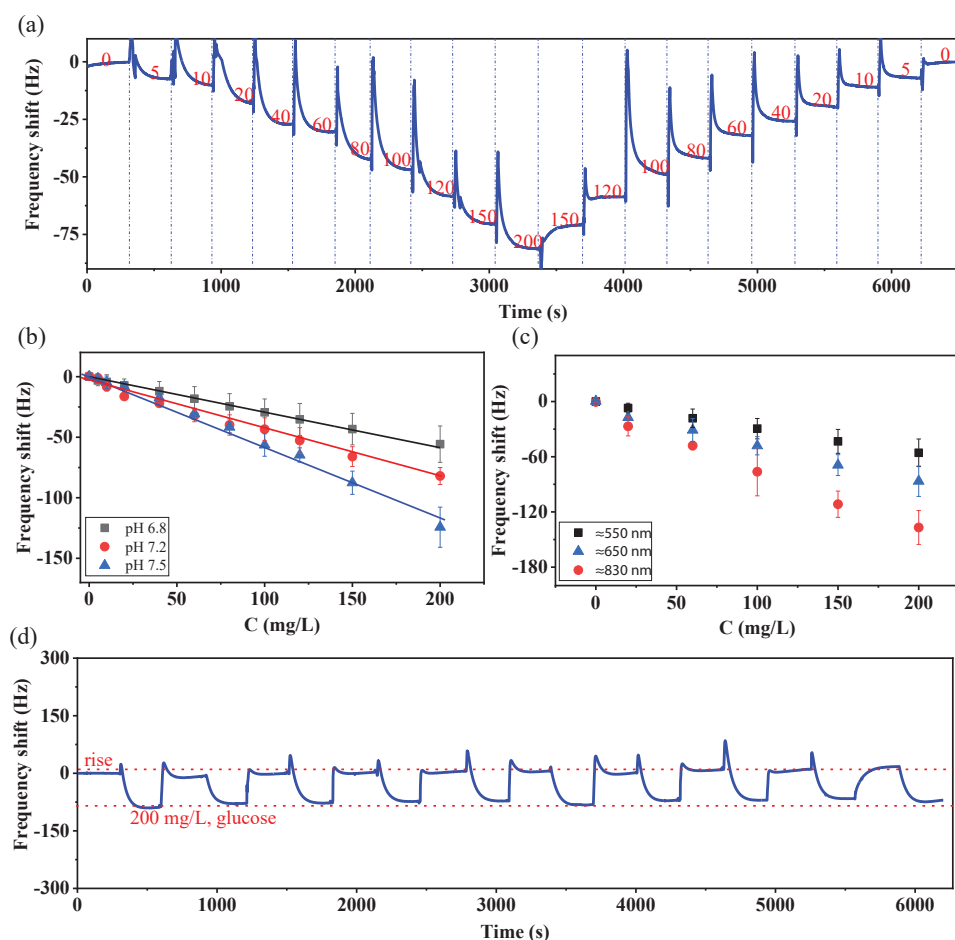


**Figure 3:** (a) The response of Au-Cys-hydrogel to glucose ranging from 0 to 200 mg/L (pH 7.2). (b) Influence of different pH on glucose test (pH 7.2). (c) The influence of different film thickness on glucose test. (d) Recovery test of Au-Cys-hydrogel (pH 7.2).

## Comparison of anti-protein performance and glucose sensitivity

Using hydrogel without Au-Cys as a control experiment, the antifouling performance of Au-Cys-hydrogel against Bovine Serum Albumin (BSA), Lysozyme (LYS), and Mucin (MUC) was evaluated, and the changes in its glucose sensitivity were analyzed. Figure 4a shows the results for BSA on both types of hydrogels. The results indicate that when the BSA concentration was 400 mg/L, the frequency shift ( $\Delta F$ ) for Hydrogel decreased by about 45 Hz; whereas, at a BSA concentration of 10,000 mg/L, the  $\Delta F$  for Au-Cys-hydrogel decreased by only about 15 Hz. Similarly, when the LYS concentration was 10 mg/L, the  $\Delta F$  for Hydrogel decreased by about 70 Hz; whereas, at a LYS concentration of 100 mg/L, the  $\Delta F$  for Au-Cys-hydrogel decreased by only about 28 Hz (Figure 4b). For mucin, when its concentration was 5 mg/L, the  $\Delta F$  for Hydrogel decreased by about 70 Hz; whereas, at a concentration of 250 mg/L, the  $\Delta F$  for Au-Cys-hydrogel decreased by only about 17 Hz (Figure 4c). In summary, compared to hydrogel without Au-Cys, the anti-protein performance of Au-Cys-hydrogel improved by approximately 25, 10, and 50 times for BSA, LYS, and MUC, respectively. These results of three proteins fully confirm that the incorporation of the antifouling material Au-Cys into the hydrogel can significantly enhance its antifouling properties. The mechanism is that Au-Cys forms a hydration layer via electrostatic and hydrogen bonding, which can bind a large number of water molecules and generate strong repulsive forces against proteins at specific distances [43,44].

Furthermore, the glucose sensitivity of Hydrogel and Au-Cys-hydrogel was compared. As shown in Figure 4d, the sensitivity of the QCM sensor was calculated based on the Sauerbrey equation, assuming that the adsorption layer on the

QCM chips is rigid and uniform. The sensitivity calculation is shown in Equation (1). When the glucose concentration was 100 mg/L, the average value of  $\Delta F$  for hydrogels containing Au-Cys was 45 Hz, while for hydrogels without Au-Cys, the average value of  $\Delta F$  was 34 Hz. Therefore, the sensitivity of glucose increased from 0.34 Hz/(mg/L) to 0.45 Hz/(mg/L). This enhancement can be attributed to the signal amplification provided by the incorporated gold nanoparticles. Collectively, these findings demonstrate that the introduction of Au-Cys not only improves the antifouling properties of the hydrogel but also enhances its sensitivity to glucose.

$$\text{Sensitivity} = \frac{\Delta F}{C} \quad (1)$$

## Conclusion

This study successfully developed a novel QCM-based glucose sensor incorporating an antifouling hydrogel. The sensor demonstrated reliable detection of salivary glucose under physiological conditions and exhibited exceptional resistance to protein fouling. Notably, the sensitivity of hydrogels without Au-Cys increased from 0.34 Hz/(mg/L) to 0.45 Hz/(mg/L) for hydrogels containing Au-Cys. Furthermore, the antifouling properties of the Au-Cys-hydrogel against bovine serum albumin, lysozyme, and mucin were significantly enhanced, improving antifouling performance by approximately 25-, 10-, and 50-fold, respectively. These findings offer valuable insights for the design of advanced antifouling QCM glucose sensors.

## Data availability statement

The data that support the findings of this study are available from the corresponding author upon reasonable request.

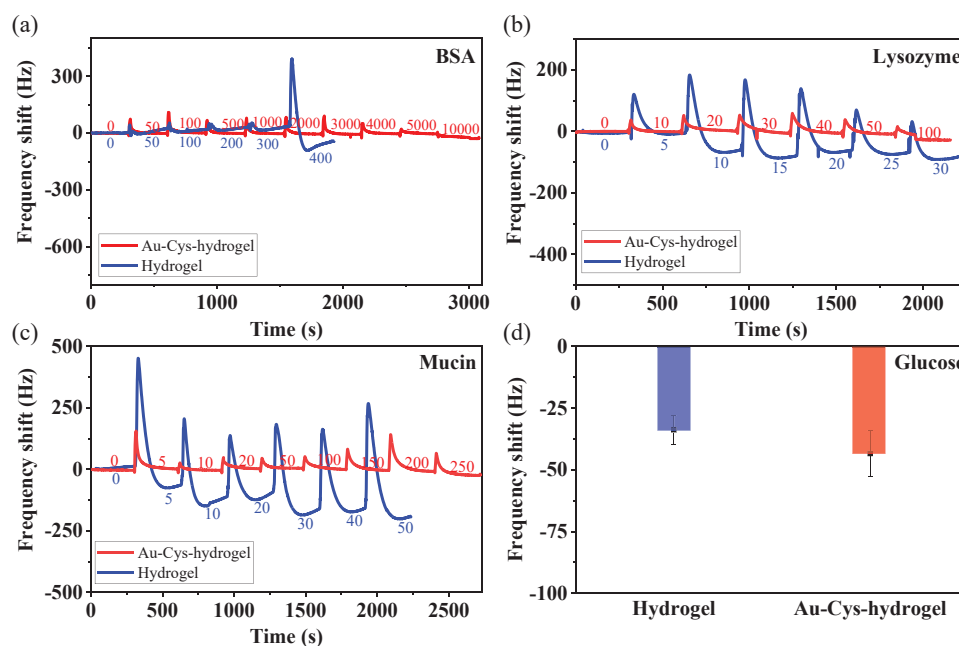


**Figure 4:** Results of tests on BSA (a), lysozyme (b), mucin (c) and glucose (d) by Au-Cys-hydrogel and hydrogel.

## Acknowledgement

This research was supported by the Special Scientific Research Project for Capital Hygiene Development (grant number 2022-2-5042), the National Natural Science Foundation of China (grant numbers L2324121, 52472156), the Institutionalization Project of Chinese Academy of Sciences (grant number JZHKYPT-2021-02), the Key Research Program of the National Natural Science Foundation of China (grant number 2021YFA1201500).

## References

- Abel ED, Gloyn AL, Evans-Molina C, Joseph JJ, Misra S, Pajvani UB, et al. Diabetes Mellitus – Progress and Opportunities in the Evolving Epidemic. *Cell*. 2024;187(15):3789-3820. Available from: <https://doi.org/10.1016/j.cell.2024.06.029>
- Antar SA, Ashour NA, Sharaky M, Khattab M, Ashour NA, Zaid RT, et al.. Diabetes Mellitus: Classification, Mediators, and Complications; A Gate to Identify Potential Targets for the Development of New Effective Treatments. *Biomed Pharmacother*. 2023;168:115734. Available from: <https://doi.org/10.1016/j.biopha.2023.115734>
- Saeedi P, Petersohn I, Salpea P, Malanda B, Karuranga S, Unwin N, et al. Global and Regional Diabetes Prevalence Estimates for 2019 and Projections for 2030 and 2045: Results from the International Diabetes Federation Diabetes Atlas, 9th Edition. *Diabetes Res Clin Pract*. 2019;157:107843. Available from: <https://doi.org/10.1016/j.diabres.2019.107843>
- Khunti K, Zaccardi F, Amod A, Aroda VR, Aschner P. Glycaemic Control Is Still Central in the Hierarchy of Priorities in Type 2 Diabetes Management. *Diabetologia*. 2025;68(1):17-28. Available from: <https://doi.org/10.1007/s00125-024-06254-w>
- Olczuk D, Priefer R. A History of Continuous Glucose Monitors (CGMs) in Self-Monitoring of Diabetes Mellitus. *Diabetes Metab Syndr Clin Res Rev*. 2018;12(2):181-187. Available from: <https://doi.org/10.1016/j.dsx.2017.09.005>
- Clarke SF, Foster JR. A History of Blood Glucose Meters and Their Role in Self-Monitoring of Diabetes Mellitus. *Br J Biomed Sci*. 2012;69(2):83-93. Available from: <https://doi.org/10.1080/09674845.2012.12002443>
- Delbeck S, Vahlsing T, Leonhardt S, Steiner G, Heise HM. Non-Invasive Monitoring of Blood Glucose Using Optical Methods for Skin Spectroscopy—Opportunities and Recent Advances. *Anal Bioanal Chem*. 2019;411(1):63-77. Available from: <https://doi.org/10.1007/s00216-018-1395-x>
- Kim J, Campbell AS, Wang J. Wearable Non-Invasive Epidermal Glucose Sensors: A Review. *Talanta*. 2018;177(August 2017):163-170. Available from: <https://doi.org/10.1016/j.talanta.2017.08.077>
- Gupta S, Sandhu SV, Bansal H, Sharma D. Comparison of Salivary and Serum Glucose Levels in Diabetic Patients. *J Diabetes Sci Technol*. 2015;9(1):91-96. Available from: <https://doi.org/10.1177/1932296814552673>
- Ngamchuea K, Batchelor-McAuley C, Compton RG. Understanding Electroanalytical Measurements in Authentic Human Saliva Leading to the Detection of Salivary Uric Acid. *Sensors Actuators, B Chem*. 2018;262:404-410. Available from: <https://doi.org/10.1016/j.snb.2018.02.014>
- Soni A, Jha SK. Smartphone Based Non-Invasive Salivary Glucose Biosensor. *Anal Chim Acta*. 2017;996:54-63. Available from: <https://doi.org/10.1016/j.aca.2017.10.003>
- Furusawa H, Sekine T, Ozeki T. Hydration and Viscoelastic Properties of High- and Low-Density Polymer Brushes Using a Quartz-Crystal Microbalance Based on Admittance Analysis (QCM-A). *Macromolecules*. 2016;49(9):3463-3470. Available from: <https://doi.org/10.1021/acs.macromol.6b00035>
- Zhang Z, Fan J, Yu J, Zheng S, Chen W, Li H, et al. New Poly(N,N-Dimethylaminoethyl Methacrylate)/Polyvinyl Alcohol Copolymer Coated QCM Sensor for Interaction with CWA Simulants. *ACS Appl Mater Interfaces*. 2012;4(2):944-949. Available from: <https://doi.org/10.1021/am201603n>
- Tsuge Y, Moriyama Y, Tokura Y, Shiratori S. Silver Ion Polyelectrolyte Container as a Sensitive Quartz Crystal Microbalance Gas Detector. *Anal Chem*. 2016;88(21):10744-10750. Available from: <https://doi.org/10.1021/acs.analchem.6b03387>
- Webster A, Vollmer F, Sato Y. Probing Biomechanical Properties with a Centrifugal Force Quartz Crystal Microbalance. *Nat Commun*. 2014;5:1-8. Available from: <https://doi.org/10.1038/ncomms6284>
- Yoo HY, Bruckenstein S. A Novel Quartz Crystal Microbalance Gas Sensor Based on Porous Film Coatings. A High Sensitivity Porous Poly(Methylmethacrylate) Water Vapor Sensor. *Anal Chim Acta*. 2013;785:98-103. Available from: <https://doi.org/10.1016/j.aca.2013.04.052>
- Zhang D, Chen H, Zhou X, Wang D, Jin Y, Yu S. In-Situ Polymerization of Metal Organic Frameworks-Derived ZnCo2O4/Polypyrrole Nanofilm on QCM Electrodes for Ultra-Highly Sensitive Humidity Sensing Application. *Sensors Actuators, A Phys*. 2019;295:687-695. Available from: <https://doi.org/10.1016/j.sna.2019.06.050>
- Ko A, Liao C. Salivary Glucose Measurement: A Holy Ground for Next Generation of Non-Invasive Diabetic Monitoring. *Hybrid Adv*. 2023;3:100052. Available from: <https://doi.org/10.1016/j.hybadv.2023.100052>
- Calixto PS, Ferraz FC, Dutra GC, Julia M, Pelozo B, Eleni M, et al. Exploring Saliva as a Sample for Non-Invasive Glycemic Monitoring in Diabetes: A Scoping Review. *Biomedicines*. 2025;13(3):713. Available from: <https://doi.org/10.3390/biomedicines13030713>
- Ngamchuea K, Chaisiwamongkhon K, Batchelor-Mcauley C, Compton RG. Chemical Analysis in Saliva and the Search for Salivary Biomarkers—a Tutorial Review. *Analyst*. 2018;143(1):81–99. Available from: <https://doi.org/10.1039/c7an01571b>
- Dou Q, Wang S, Zhang Z, Wang Y, Zhao Z, Guo H, et al. Nanoscale A Highly Sensitive Quartz Crystal Microbalance Sensor Modified with Antifouling Microgels for Saliva Glucose Monitoring. *Nanoscale*. 2020;12:19317–19324. Available from: <https://doi.org/10.1039/d0nr03193c>
- Yang W, Xue H, Carr LR, Wang J, Jiang SZ. Zwitterionic Poly(Carboxybetaine) Hydrogels for Glucose Biosensors in Complex Media. *Biosens Bioelectron*. 2011;26(5):2454–2459. Available from: <https://doi.org/10.1016/j.bios.2010.10.031>
- Hu Y, Liang B, Fang L, Ma G, Yang G, Zhu Q, et al. Antifouling Zwitterionic Coating via Electrochemically Mediated Atom Transfer Radical Polymerization on Enzyme-Based Glucose Sensors for Long-Time Stability in 37°C Serum. *Langmuir*. 2016;32(45):11763–11770. Available from: <https://doi.org/10.1021/acs.langmuir.6b03016>
- Banerjee I, Pangule RC, Kane RS. Antifouling Coatings: Recent Developments in the Design of Surfaces That Prevent Fouling by Proteins, Bacteria, and Marine Organisms. *Adv Mater*. 2011;23(6):690–718. Available from: <https://doi.org/10.1002/adma.201001215>
- Sabaté del Río J, Henry OYF, Jolly P, Ingber DE. An Antifouling Coating That Enables Affinity-Based Electrochemical Biosensing in Complex Biological Fluids. *Nat Nanotechnol*. 2019;14(12):1143–1149. Available from: <https://doi.org/10.1038/s41565-019-0566-z>
- Dou Q, Zhang Z, Wang Y, Wang S, Hu D, Zhao Z, et al. Ultrasensitive Poly(Boric Acid) Hydrogel-Coated Quartz Crystal Microbalance Sensor by Using UV Pressing-Assisted Polymerization for Saliva Glucose Monitoring. *ACS Appl Mater Interfaces*. 2020;12:34190–34197. Available from: <https://doi.org/10.1021/acsami.0c08229>



27. Zhang P, Jain P, Tsao C, Yuan Z, Li W, Li B, et al. Polypeptides with High Zwitterion Density for Safe and Effective Therapeutics. *Angew Chem Int Ed.* 2018;57(26):7743–7747. Available from: <https://doi.org/10.1002/anie.201802452>
28. Gu G, Yang X, Li Y, Guo J, Huang J. Advanced Zwitterionic Polymeric Membranes for Diverse Applications Beyond Antifouling. *Sep Purif Technol.* 2025;356:129848. Available from: <https://doi.org/10.1016/j.seppur.2024.129848>
29. Zheng C, Hussain Z, Chen C, Jan R, Haas D. One-Step Antifouling Coating of Polystyrene Using Engineered Polypeptides. *J Colloid Interface Sci.* 2025;685:350–360. Available from: <https://doi.org/10.1016/j.jcis.2025.01.147>
30. Alswehleh AM, Cheng N, Canton I, Ustbas B, Xue X, Ladmira V, et al. Zwitterionic Poly(Amino Acid Methacrylate) Brushes. *J Am Chem Soc.* 2014;136(26):9404–9413. Available from: <https://doi.org/10.1021/ja503400r>
31. Chen S, Jiang S. A New Avenue to Nonfouling Materials. *Adv Mater.* 2008;20(2):335–338. Available from: <https://doi.org/10.1002/adma.200701164>
32. Cao F, Huang Y, Wang F, Kwak D, Dong Q, Song D, et al. A High-Performance Electrochemical Sensor for Biologically Meaningful L-Cysteine Based on a New Nanostructured L-Cysteine Electrocatalyst. *Anal Chim Acta.* 2018;1019:103–110. Available from: <https://doi.org/10.1016/j.aca.2018.02.04>
33. Zarei K, Ghorbani M. Fabrication of a New Ultrasensitive AuNPs-MIC-Based Sensor for Electrochemical Determination of Streptomycin. *Electrochim Acta.* 2019;299:330–338. Available from: <https://doi.org/10.1016/j.electacta.2019.01.016>
34. Dong H, Zou F, Hu X, Zhu H, Koh K, Chen H. Analyte Induced AuNPs Aggregation Enhanced Surface Plasmon Resonance for Sensitive Detection of Paraquat. *Biosens Bioelectron.* 2018;117:605–612. Available from: <https://doi.org/10.1016/j.bios.2018.06.057>
35. Perni S, Prokopovich P. RSC Advances Nanocarriers. *RSC Adv.* 2014;4:51904–51910. Available from: <https://doi.org/10.1039/C4RA10023A>
36. Peng H, Ning X, Wei G, Wang S, Dai G, Ju A. The Preparations of Novel Cellulose/Phenylboronic Acid Composite Intelligent Bio-Hydrogel and Its Glucose, PH-Responsive Behaviors. *Carbohydr Polym.* 2018;195:349–355. Available from: <https://doi.org/10.1016/j.carbpol.2018.04.119>
37. Mikhlin Y, Likhatski M, Tomashevich Y, Romanchenko A, Erenburg S, Trubina S. Journal of Electron Spectroscopy and XAS and XPS Examination of the Au–S Nanostructures Produced via the Reduction of Aqueous Gold (III) by Sulfide Ions. *J Electron Spectrosc Relat Phenomena.* 2010;177(1):24–29. Available from: <https://doi.org/10.1016/j.elspec.2009.12.007>
38. Chenakin SP, Kruse N. Au 4f Spin–Orbit Coupling Effects in Supported Gold Nanoparticles. *Phys Chem Chem Phys.* 2016;18:22778–22782. Available from: <https://doi.org/10.1039/c6cp03362h>
39. Mitsumori M, Yamaguchi M, K. Y. A New Approach to Noninvasive Measurement of Blood Glucose Using Saliva Analyzing System. *Proceedings of the 20th Annual International Conference of the IEEE Engineering in Medicine and Biology Society.* 1998;20(4):1767–1770.
40. Yamaguchi M, Mitsumori MKY. Noninvasively Measuring Blood Glucose Using Saliva. *IEEE Eng Med Biol Mag.* 1998;17(3):59–63. Available from: <https://doi.org/10.1109/51.677170>
41. Shinen MH, Essa FO, Naji AS. Study the Sensitivity of Quartz Crystal Microbalance (QCM) Sensor Coated with Different Thickness of Polyaniline for Determination Vapors of Ether, Chloroform, Carbon Tetrachloride, and Ethyl Acetate. *Chem Mater Res.* 2014;6(3):7–12. Available from: <https://iiste.org/Journals/index.php/CMR/article/view/11709>
42. Wang J, Wang Z, Yu J, Kahkoska AR, Buse JB, Gu Z. Glucose-Responsive Insulin and Delivery Systems: Innovation and Translation. *Adv Mater.* 2020;32(13):1–19. Available from: <https://doi.org/10.1002/adma.201902004>
43. Chou YN, Chang Y, Wen TC. Applying Thermosettable Zwitterionic Copolymers as General Fouling-Resistant and Thermal-Tolerant Biomaterial Interfaces. *ACS Appl Mater Interfaces.* 2015;7(19):10096–100107. Available from: <https://doi.org/10.1021/acsami.5b01756>
44. Escobar IC, Van Der Bruggen B. Microfiltration and Ultrafiltration Membrane Science and Technology. *J Appl Polym Sci.* 2015;132(21):42002. Available from: <https://doi.org/10.1002/app.42002>

## Discover a bigger Impact and Visibility of your article publication with Peertechz Publications

### Highlights

- ❖ Signatory publisher of ORCID
- ❖ Signatory Publisher of DORA (San Francisco Declaration on Research Assessment)
- ❖ Articles archived in worlds' renowned service providers such as Portico, CNKI, AGRIS, TDNet, Base (Bielefeld University Library), CrossRef, Scilit, J-Gate etc.
- ❖ Journals indexed in ICMJE, SHERPA/ROMEO, Google Scholar etc.
- ❖ OAI-PMH (Open Archives Initiative Protocol for Metadata Harvesting)
- ❖ Dedicated Editorial Board for every journal
- ❖ Accurate and rapid peer-review process
- ❖ Increased citations of published articles through promotions
- ❖ Reduced timeline for article publication

Submit your articles and experience a new surge in publication services

<https://www.peertechzpublications.org/submission>

Peertechz journals wishes everlasting success in your every endeavours.